Density Functional Theory Study of Lithium Diffusion at the Interface between Olivine-type $LiFePO_4$ and $LiMnPO_4$

Jianjian Shi, [1] Zhiguo Wang,[1*] Yong Qing Fu[1,2*]

1 School of Physical Electronics, Center for Public Security Information and Equipment Integration Technology, University of Electronic Science and Technology of China, Chengdu, 610054, P.R. China
2 Faculty of Engineering and Environment, University of Northumbria, Newcastle upon Tyne, NE1 8ST, UK

[*]Corresponding author. E-mail: zgwang@uestc.edu.cn (ZW); richard.fu@northumbria.ac.uk (YF)

Abstract:

Coating $LiMnPO_4$ with a thin layer of $LiFePO_4$ shows a better electrochemical performance than the pure $LiFePO_4$ and $LiMnPO_4$, thus it is critical to understand Li diffusion at their interfaces to improve the performance of electrode materials. Li diffusion at the $(100)_{LiFePO4}//(100)_{LiMnPO4}$, $(010)_{LiFePO4}//(010)_{LiMnPO4}$, and $(001)_{LiFePO4}//(001)_{LiMnPO4}$ interfaces between $LiFePO_4$ and $LiMnPO_4$ was investigated using density functional theory. The calculated diffusion energy barriers are 0.55 eV for Li to diffuse along the (001) interface, 0.44 and 0.49 eV for the Li diffusion inside the $LiMnPO_4$ and along the (100) interface, respectively. When the Li diffuses from the $LiFePO_4$ to $LiMnPO_4$ by passing through the (010) interfaces, the diffusion barriers are 0.45 and 0.60 eV for the Li diffusions in both sides. The diffusion barriers for the Li to diffuse in $LiMnPO_4$ near the interfaces decrease compared with those in the pure $LiMnPO_4$. The calculated diffusion coefficient of Li along the (100) interface is in the range of 3.65×10^{-11}-5.28×10^{-12} cm^2/s, which is larger than that in the pure $LiMnPO_4$ with a value of 7.5×10^{-14} cm^2/s. Therefore, the charging/discharging rate performance of the $LiMnPO_4$ can be improved by surface coating with the $LiFePO_4$.

Keywords: Interfaces; diffusion; density functional theory

1. Introduction

Lithium ion batteries (LIBs) have attracted much attention due to their wide applications in electric vehicles and portable electronic devices. Different materials are currently investigated to improve the overall performance of the LIBs. Good candidates of the LIBs must demonstrate high level of safety, low price, durability, long cycle life and high energy density. Among them, the olivine group materials, i.e., $LiMPO_4$ (M=Fe, Co, Ni, Mn), are known to be promising cathode materials for the LIBs. $LiFePO_4$, one of the most prominent members of this group materials, has received extensive interest as storage cathodes because of its low raw material cost, environmental friendliness, safety, and good cycle stability [1-4]. The olivine structure of the $LiFePO_4$ is a hexagonal close packed array of oxide ions containing isolated PO_4 tetrahedral and corner-sharing FeO_6 octahedral in the (011) plane and edge-sharing LiO_6 octahedral, stacked along the [010] direction. Because the oxygen atoms are strongly bonded to both Fe and P atoms, the structure of the $LiFePO_4$ is more stable at high temperatures than many other layered oxides, such as $LiMnO_2$. $LiFePO_4$ was reported to be stable up to 400 °C [5, 6]. The good lattice stability results in excellent cyclic performance and operation safety. However, the strong covalent oxygen bonds in the $LiFePO_4$ also lead to a low intrinsic conductivity at room temperature (~10^{-9} S/cm) and low value of Li diffusion coefficient (~10^{-14} cm^2/s), thus resulting in a poor rate capability. Currently, the relatively low conductivity and poor Li transport properties can be improved by reducing crystal size and changing the microstructure/morphology, using surface modification and forming composite structures. Using these various methods, the electronic conductivity and Li diffusion coefficients can be increased up to 10^{-1} S/cm and 10^{-9} cm^2/s, respectively [7-16]. Another drawback of the $LiFePO_4$ is its relatively small voltage (3.4 V vs. Li^+/Li^0), which limits the maximum energy density generated.

$LiCoPO_4$ and $LiNiPO_4$ have higher output voltages (4.8 and 5.1 V, respectively, vs. Li^+/Li^0) in the phosphate frameworks, which exceed the stability window of most commercial liquid electrolytes. $LiMnPO_4$ has a voltage of 4.1 eV, which makes it also attractive, because this voltage value is considered to be the maximum limit for most liquid electrolytes and larger than that of the $LiFePO_4$. However, compared to the $LiFePO_4$, electrochemical performance of the $LiMnPO_4$ as the cathode material for the LIBs is poorer, therefore, various methods have been applied to solve this problem, such as doping modification or reducing the crystal size down to hundreds or even tens of nanometers [10, 17-19]. However, even after applying these methods, it still cannot meet the requirements for fast charging/discharging rate. A good way to solve this problem is to coat the $LiMnPO_4$ with carbon (C) [20]. Unfortunately, the C coated $LiMnPO_4$ turned out to be more problematic than that of $LiFePO_4$ because the C is less reactive with Mn than with Fe, thus adhesion becomes poorer [21]. Therefore, a good idea was proposed to use the solid solution $LiMn_xFe_{1-x}PO_4$, with its intermediate composition to be the best compromise, and take advantage of the Mn^{2+}/Mn^{3+} redox potential without losing too much in the cycling life and power [22]. Recently coating $LiMnPO_4$ with a thin layer of $LiFePO_4$ was proposed to take benefit of the catalytic reaction of Fe with C, which could open a new route to improve the performance of the olivine family as the cathode materials for LIBs [23]. The composite has been proven to show a better electrochemical performance [23].

For these multilayer cathodes, Li diffusion from one site to another needs to pass through adjacent PO_4 tetrahedral sites and FeO_6 (MnO_6) octahedral sites by a hopping mechanism. Atomistic modeling simulation can help to clarify the diffusion route of the Li in the olivine-type cathode-active materials. Previous studies revealed that lithium diffusion is a one-dimensional motion along the [010] direction of $LiMPO_4$, and the diffusion barriers are much higher in the

other directions [24]. Experimentally, the one-dimensional diffusion path was directly detected by means of high-temperature powder neutron diffraction combined with a maximum entropy method [25]. When $LiMnPO_4$ particles are coated with $LiFePO_4$, Li will need to diffuse through the interface between the $LiMnPO_4$ and $LiFePO_4$. It is critical to understand the difference between the Li diffusions though interfaces and within the bulk materials, which will provide strategies to further improve the performance of electrode materials. In the present work, we report the density functional theory (DFT) study on Li ion diffusion at the interface between the $LiMnPO_4$ and $LiFePO_4$.

2. Simulation methodology

DFT calculations were performed using the SIESTA (Spanish Initiative for Electronic Simulations with Thousands of Atoms) Package [26, 27]. A linear combination of numerical localized atomic orbital basis sets was used for the description of valence electrons [28]. Electron-ion interaction and electron exchange-correlation were described by norm-conserving pseudopotentials [28] and the local-density approximation for the exchange correlation term [29], as proposed by Perdew and Zunger [30], respectively. The spin-polarization was considered for all the calculations. The valence electron wave functions were expanded using a DZP basis set (a double-ζ basis set plus polarization functional). An energy cut-off was set to be 150 Ry.

The unit cell of $LiMPO_4$ (M = Mn or Fe) was composed of 4 Li atoms, 4 M atoms, 4 P atoms and 16 O atoms. The geometric optimization of the unit cell was performed using a conjugate gradient method until the maximum force was less than 0.02 eV/Å. The relaxed atomic structures for unit cells of the $LiFePO_4$ and $LiMnPO_4$ are shown in Figs. 1a and 1b, respectively. A 6×4×2 Monkhorst-Pack [31] mesh was used for the k-point sampling. The surface properties of the

$LiFePO_4$ and $LiMnPO_4$ have been previously studied using the first principle calculations [32, 33]. It was reported that (100) and (010) surfaces are low energy surfaces, whereas the (001) surface has a higher surface energy than those of the (100) and (010) surfaces [32, 33]. In the present work, $(100)_{LiFePO4}//(100)_{LiMnPO4}$, $(010)_{LiFePO4}//(010)_{LiMnPO4}$, and $(001)_{LiFePO4}//(001)_{LiMnPO4}$ interfaces between $LiFePO_4$ and $LiMnPO_4$ were investigated. The (001) interface model was built by $[3(a_1+a_2)/2]\times[2(b_1+b_2)/2]\times(c_1+c_2)$ with half of the box filled with $LiFePO_4$ and the rest part filled with $LiMnPO_4$. It contains 336 atoms, and a_1, b_1, c_1 and a_2, b_2, c_2 are the lattice constants of the $LiFePO_4$ and $LiMnPO_4$, respectively. An average lattice constant was used to model the lattice constant parallel to the interfaces of this heterostructure. The relaxed atomistic configurations are shown in Fig. 2a. Using the same method, the (100) and (010) interface models were built with $[3(a_1+a_2)]\times[2(b_1+b_2)/2]\times[(c_1+c_2)/2]$ and $[3(a_1+a_2)/2]\times[(b_1+b_2)]\times[(c_1+c_2)/2]$, respectively, which contain 336 and 168 atoms, respectively. The relaxed atomistic configurations of the (010) and (100) interface models are shown in Figs. 2b and 2c, respectively. A 2×2×2 k-point grid within the Monkhorst-Pack scheme was used to sample the Brillouin zone in the interface models.

As the electrochemical behavior of LIBs is based on the diffusion of Li ions, atomic defects, such as vacancies and antisite defects, can significantly affect the Li ion diffusion [34]. Antisite defects are commonly existed in the $LiMPO_4$ and have been verified by experimental observations [35-37] [38]. These anti-site defects were reported to block the diffusion of Li ions [39, 40]. The interfaces also act as defect sink of materials, i.e. the defects prefer to segregate to the interface, thus affect the diffusivity of Li ions. In this work, we focused on the effect of interface on the diffusion of Li ion, and used defect-free crystals to model the interfaces.

Huge computation effort is needed to investigate the diffusion profile in the large cell of the interface model with a nudged elastic band (NEB) [41] method. In this work, a constrained method was used to determine the diffusion profiles of Li in the interface, in which the Li ion was pushed along the diffusion path by constraining it in the direction along the path. One degree of freedom of the Li ion was fixed, while all the other n-1 degrees of freedom were allowed to relax, i.e. the energy of the system was minimized in an n-1 dimensional hyperplane. The energy profile of the Li ion was obtained by small stepwise increments of the fixed coordinate from the initial to the final positions [42]. In this work, the y coordinate of Li was fixed due to the one-dimensional diffusion characteristics along the [010] direction in the olivine-type materials [24]. We have compared the diffusion barriers of Li in a pure $LiMPO_4$ obtained by the constrained method in a 3a×2b×c supercell from the literatures, and the results showed that the constrained method is effective to study the diffusion behavior in the $LiMPO_4$.

3. Results and discussion

The optimized lattice constants for the $LiFePO_4$ and $LiMnPO_4$ are summarized in Table 1, along with other theoretical results and experimental values. The calculated values are smaller than the experimental ones, but the errors of the computed values compared with the experimental ones are within 0.64-1.94% [10, 43]. The underestimation of the lattice constant compared with the equilibrium values is due to the feature of LDA functional used [44]. The lattice constants of the $LiFePO_4$ and $LiMnPO_4$ are very close to each other, so the average lattice constants used to model the lattice constants parallel to the interface of heterostructure is reasonably good.

We firstly compute the diffusion barriers of the Li in a pure $LiMPO_4$ obtained using the constrained method with a 3a×2b×c supercell. In the olivine $LiMPO_4$, Li atoms occupy the octahedral 4a sites [45]. The migration of one Li atom along the [010] direction in a fully lithiated $LiMPO_4$ is through the vacancy mechanism. The calculated diffusion energy barriers in the bulk $LiFePO_4$ and $LiMnPO_4$ are 0.48 and 0.60 eV, respectively, which are close to the reported values of 0.48-0.65 eV in $LiFePO_4$ [24, 34] and 0.62 eV in $LiMnPO_4$ [24] obtained using the NEB methods. They agree with experimental values of 0.54 eV for the $LiFePO_4$ [46] and 0.65 eV for the $LiMnPO_4$ [47]. The results show that diffusion energy barriers obtained using the constrained method are reasonably good. Results also suggest that Li diffusion is easier in the bulk $LiFePO_4$ than that in the $LiMnPO_4$, which is consistent with the literature [10, 24, 34, 46-48].

Due to the one-dimensional diffusion characteristics along [010] direction in the olivine-type materials [24], Li diffuses along both the (100) and (001) interfaces between the $LiFePO_4$ and $LiMnPO_4$, whereas it diffuses across the (010) interface between the $LiFePO_4$ and $LiMnPO_4$. The calculated diffusion energy barrier curves are shown in Fig. 3a, in which the blue and green dotted lines represent the diffusion barrier values of the Li in the bulk $LiFePO_4$ and $LiMnPO_4$, respectively, and the corresponding diffusion paths are shown in Figs. 3b-3d. The corresponding diffusion channels are also shown in Fig. 2. The two cases for the Li to diffuse along the (001) interface and through the (010) interfaces are illustrated in Figs. 2a and 2b, respectively. Li interacts with the atoms from both the $LiFePO_4$ and $LiMnPO_4$ when it diffuses along the channel D (see Fig. 2a), whereas it interacts with the atoms in $LiMnPO_4$ as it diffuses along the channel E (see Fig. 2b). Therefore, we define the Li diffusion paths along the (100) interface between the $LiFePO_4$ and $LiMnPO_4$ and inside the $LiMnPO_4$ using those of Li diffusions along the channels

D and E, respectively. The diffusion barrier is 0.55 eV for the Li diffuses along the (001) interface, which is in the range between those of the Li ions in both the $LiFePO_4$ and $LiMnPO_4$. As the Li diffuses along the (100) interface, the calculated diffusion barriers are 0.44 and 0.49 eV for the Li diffusion inside the $LiMnPO_4$ and along the (100) interface, respectively. The diffusion behavior of the Li along the (100) interface in the $LiFePO_4$ side is not affected by the existence of interface, but the diffusion barrier decreases with 0.16 eV in the $LiMnPO_4$ side near the interface. As the Li diffuses from $LiFePO_4$ to $LiMnPO_4$ by passing through the (010) interface, the diffusion barriers are 0.45 and 0.60 eV, which are close to those of Li diffusion in the pure $LiFePO_4$ (0.48 eV) and $LiMnPO_4$ (0.60 eV), respectively. The diffusion of the Li by passing through the (010) interface is apparently not affected. However, diffusion of the Li can be improved by forming both (100) and (001) interfaces between the $LiMnPO_4$ and $LiFePO_4$.

It is known that the strain plays an important role in the mobility of Li ions. The volume of the $FePO_4$ is increased by about 5% upon lithium intercalation, and this strain can facilitate the diffusion of Li at the interface between the $FePO_4$ and $LiFePO_4$ [39]. The same phenomenon was also observed in the lithiation process of $MnPO_4$ [49]. It was reported that the tensile strain induces the increase of Li ion mobility because the larger space induced by the volume expansion allows the Li ion to migrate easily, whereas the compressive strain causes the decrease of Li ion mobility [50]. We have calculated the strains at the interfaces between the $LiFePO_4$ and $LiMnPO_4$ and the results are listed in Table II. Clearly both tensile and compressive strains exist in the $LiFePO_4$ and $LiMnPO_4$. The lattice strain along the [010] direction is a key factor that controls the Li ion diffusion. Above results show that there is no lattice strain b at the (010) interface, and the diffusion of Li through the (010) interface is unaffected. The lattice strains

along [010] and [001] directions for the (100) interface are larger than those along the other interfaces, which induces the smaller diffusion barriers for the Li ions.

The partial density of states (PDOS) of the bulk $LiFePO_4$ and $LiMnPO_4$ are shown in Figs. 4a and 4b, respectively. For the bulk $LiFePO_4$, it is obvious that the electronic states around the Fermi level are mainly originated from Fe 3d and O 2p. Spin-up and spin-down orbital parts are significantly split around the Fermi level of the Fe 3d state. The spin-up orbital part has been fully filled. Whereas for the spin-down orbital, only the peak at 0.53 eV below the Fermi level is filled, and the others are empty. For the bulk $LiMnPO_4$, the contribution of the valence band (VB) is from Mn 3d states and O 2p states. The calculated band-gaps are 0.23 eV and 2.0 eV for the $LiFePO_4$ and $LiMnPO_4$, respectively, which agree well with the previous simulation results of 0.2 eV [51] for the $LiFePO_4$ and 2.0 eV [22, 51] for the $LiMnPO_4$. The PDOSs of the (100), (010) and (001) interfaces between the $LiFePO_4$ and $LiMnPO_4$ are shown in Figs. 4c, 4d and 4e, respectively, and they have the similar characteristics. The electronic states near the Fermi level come from the Fe 3d, Mn 3d and O 2p states. Spin-up and spin-down orbital parts are split around the Fermi level of the Fe 3d state. The spin-up orbitals have been fully filled, whereas only the states of spin-down orbitals below the Fermi level are filled, and the others are empty. From Figs. 4c, 4d and 4e, it can be seen that the VB from the Mn 3d is lower than that from the Fe 3d in energy, which agrees with the less electronegativity of Mn [52].

The working mechanism of the olivine-type cathode materials is based on the M^{2+}/M^{3+} redox reaction. For the fully lithiated $LiFePO_4$ and $LiMnPO_4$, Fe and Mn are all with 2^+ states. The diffusion mechanism of the Li is through vacancy migration. When vacancy diffusion of the Li ion occurs in the $LiMnPO_4$, the Mn^{2+} will be oxidized into Mn^{3+} state. When Fe^{2+} exists at the position near the Mn^{3+}, a charge transfer from the Fe^{2+} to Mn^{3+} occurs because the Fe has a

larger electronegative value than that of Mn. The charge transfer will induce the softening of the lattice [53], thus assisting the Li ion diffusion. Therefore, the diffusion barrier decreases with 0.16 eV in the $LiMnPO_4$ side near the interface between $LiFePO_4$ and $LiMnPO_4$.

Based on the hopping mechanism, diffusion coefficients of Li ion can be obtained from transition state theory [54] through:

$$D = a^2 v_0 \exp(-E_{diff} / k_B T) \quad (1)$$

where a is the hopping length, which is ~3 Å in the $LiFePO_4$ and $LiMnPO_4$ for the Li diffusion along the [010] direction; v_0 is the vibrational frequency of the migrating Li atom in the lattice, which is ~10^{12} Hz [54]; E_{diff} is the diffusion barriers; k_B and T are the Boltzmann constant and absolute temperature. The calculated energy barriers and diffusion coefficients in the bulk $LiFePO_4$, $LiMnPO_4$ and their interfaces are listed in Table III. Using the calculated diffusion barriers of 0.48 and 0.60 eV for Li diffusion in the $LiFePO_4$ and $LiMnPO_4$, the obtained diffusion coefficients are 7.8×10^{-12} and 7.5×10^{-14} cm^2/s, which are within the experimentally obtained data of 10^{-9}-10^{-14} cm^2/s for $LiFePO_4$ [7-9] and 4.31-8.46×10^{-14} cm^2/s for $LiMnPO_4$ [18], respectively.

The diffusion barriers of the Li at the interfaces between the $LiFePO_4$ and $LiMnPO_4$ are lower than that in the $LiMnPO_4$, for example, the diffusion barriers are 0.44 and 0.49 eV in the $LiMnPO_4$ side and along the (100) interface, compared with 0.60 eV for that within the bulk $LiMnPO_4$. The diffusion coefficients at the (100) interfaces between the $LiFePO_4$ and $LiMnPO_4$ are in the range of 3.65×10^{-11}-5.28×10^{-12} cm^2/s. The diffusivity of the Li ion in the $LiMnPO_4$ is the key factor (which has the largest diffusion energy barrier of 0.60 eV) determining the charging/discharging rate of the composite. Our results clearly showed that the existence of

interfaces can reduce the diffusion energy barrier. Therefore, charging/discharging rate performance of the $LiMnPO_4$ could be improved by forming interfaces with the $LiFePO_4$.

For further exploration, C coating is an effective way to increase the electrode conductivity, improve the surface chemistry of the active material, and protect the electrode from direct contact with electrolyte, thus leading to an enhanced cycle life of the batteries [20]. However, carbon coating has different effects when it is deposited onto the $LiMnPO_4$ and $LiFePO_4$, respectively. As the C coating on the $LiFePO_4$ is more effective than that on the $LiMnPO_4$ due to the less reactivity of the C with Mn than with Fe [21], the core/shell structure of $LiMnPO_4$/$LiFePO_4$/C would be better than $LiMnPO_4$/C to be used to improve the performance of the olivine structure materials being used as the cathode for LIBs.

4. Conclusions

Electronic structures and lithium diffusion were investigated for the (001), (010) and (100) interfaces between $LiMnPO_4$ and $LiFePO_4$ using first principles calculation methods. The calculated diffusion energy barriers of the bulk $LiFePO_4$ and $LiMnPO_4$ are 0.48 and 0.60 eV, respectively. The diffusion barrier is 0.55 eV for Li diffuses along the (001) interface, 0.44 and 0.49 eV for the Li diffusion inside the $LiMnPO_4$ and along the (100) interface, respectively. As Li diffuses from $LiFePO_4$ to $LiMnPO_4$ by passing through the (010) interfaces, the diffusion barriers are 0.45 and 0.60 eV. The diffusion barriers along the (010) and (001) interfaces are lower than that in the pure $LiMnPO_4$. The calculated diffusion coefficients of Li in (100) interface is in the range of 3.65×10^{-11}-5.28×10^{-12} cm^2/s, which is larger than that in the pure $LiMnPO_4$ with a value of 7.5×10^{-14} cm^2/s. Therefore, it can be concluded that the

charging/discharging rate performance of $LiMnPO_4$ is improved by surface coating with $LiFePO_4$.

Acknowledgement:

This work was financially supported by the National Natural Science Foundation of China (11474047). Funding support from Royal academy of Engineering UK-Research Exchange with China and India is acknowledged. This work was carried out at National Supercomputer Center in Tianjin, and the calculations were performed on TianHe-1(A).

References:

[1] Ellis B L, Lee K T and Nazar L F 2010 Chem. Mater. **22** 691-714

[2] Zhao Y, Peng L L, Liu B R and Yu G H 2014 Nano Lett. **14** 2849-53

[3] Wu S, Chen M, Chien C and Fu Y 2009 J. Power Sources **189** 440-4

[4] Harrison K L and Manthiram A 2011 Inorg. Chem. **50** 3613-20

[5] Arnold G, Garche J, Hemmer R, Strobele S, Vogler C and Wohlfahrt-Mehrens A 2003 J. Power Sources **119** 247-51

[6] Takahashi M, Tobishima S, Takei K and Sakurai Y 2002 Solid State Ionics **148** 283-9

[7] Yang S, Zhou X, Zhang J and Liu Z 2010 J. Mater. Chem. **20** 8086

[8] Tang K, Yu X, Sun J, Li H and Huang X 2011 Electrochim. Acta **56** 4869-75

[9] Trócoli R, Franger S, Cruz M, Morales J and Santos-Peña J 2014 Electrochim. Acta **135** 558-67

[10] Di Lecce D and Hassoun J 2015 J. Phys. Chem. C **119** 20855-63

[11] Zhang H, Xu Y L, Zhao C J, Yang X and Jiang Q 2012 Electrochim. Acta **83** 341-7

[12] Doeff M M, Hu Y Q, McLarnon F and Kostecki R 2003 Electrochem. Solid St. **6** A207-A9

[13] Hsu K F, Tsay S Y and Hwang B J 2004 J. Mater. Chem. **14** 2690-5

[14] Ravet N, Chouinard Y, Magnan J F, Besner S, Gauthier M and Armand M 2001 J. Power Sources **97-8** 503-7

[15] Ellis B, Kan W H, Makahnouk W R M and Nazar L F 2007 J. Mater. Chem. **17** 3248

[16] Padhi A K, Nanjundaswamy K S, Masquelier C, Okada S and Goodenough J B 1997 J. Electrochem. Soc. 144 1609-13

[17] Gan Y, Chen C, Liu J, Bian P, Hao H and Yu A 2015 J. Alloy. Comp. **620** 350-7

[18] Zhang Z, Hu G, Cao Y, Duan J, Du K and Peng Z 2015 Solid State Ionics **283** 115-22

[19] Drezen T, Kwon N-H, Bowen P, Teerlinck I, Isono M and Exnar I 2007 J. Power Sources **174** 949-53

[20] Li H and Zhou H 2012 Chem. Commun. **48** 1201-17

[21] Ravet N, Gauthier M, Zaghib K, Goodenough J B, Mauger A, Gendron F and Julien C M 2007 Chem. Mater. **19** 2595-602

[22] Yamada A and Chung S-C 2001 J. The Electrochem. Soc. **148** A960

[23] Zaghib K, Trudeau M, Guerfi A, Trottier J, Mauger A, Veillette R and Julien C M 2012 J. Power Sources **204** 177-81

[24] Fisher C A J, Prieto V M H and Islam M S 2008 Chem. Mater. **20** 5907-15

[25] Nishimura S, Kobayashi G, Ohoyama K, Kanno R, Yashima M and Yamada A 2008 Nat. Mater. **7** 707-11

[26] Perdew J P, Burke K and Ernzerhof M 1996 Phys. Rev. Lett. **77** 3865-8

[27] Soler J M, Artacho E, Gale J D, Garcia A, Junquera J, Ordejon P and Sanchez-Portal D 2002 J. Phys.-Condens. Mat. **14** 2745-79

[28] Troullier N and Martins J L 1991 Phys. Rev. B **43** 1993-2006

[29] Ceperley D M and Alder B J 1980 Phys. Rev. Lett. **45** 566-9

[30] Perdew J P and Zunger A 1981 Phys. Rev. B **23** 5048-79

[31] Pack J D and Monkhorst H J 1977 Phys. Rev. B **16** 1748-9

[32] Wang L, Zhou F, Meng Y S and Ceder G 2007 Phys. Rev. B **76** 165435

[33] Wang L, Zhou F and Ceder G 2008 Electrochem. Solid State Lett. **11** A94-A6

[34] Hoang K and Johannes M 2011 Chem. Mater. **23** 3003-13

[35] Chung S-Y, Choi S-Y, Yamamoto T and Ikuhara Y 2008 Phys. Rev. Lett. **100** 125502

[36] Chung S-Y, Choi S-Y, Lee S and Ikuhara Y 2012 Phys. Rev. Lett. **108** 195501

[37] Paolella A, Turner S, Bertoni G, Hovington P, Flacau R, Boyer C, Feng Z, Colombo M, Marras S, Prato M, Manna L, Guerfi A, Demopoulos G P, Armand M and Zaghib K 2016 Nano Lett. **16** 2692-7

[38] Devaraju M K, Truong Q D, Hyodo H, Sasaki Y and Honma I 2015 Sci. Rep. **5** 11041

[39] Dathar G K P, Sheppard D, Stevenson K J and Henkelman G 2011 Chem. Materials **23** 4032-7

[40] Hu B and Tao G 2015 J. Mater. Chem. A **3** 20399-407

[41] Henkelman G, Uberuaga B P and Jonsson H 2000 J. Chem. Phys. **113** 9901-4

[42] Sensato F R, Gracia L, Beltrán A, Andrés J and Longo E 2012 J. Phys. Chem. C **116** 16127-37

[43] Xu Y-N 2004 J. Appl. Phys. **95** 6583

[44] Perdew J P, Chevary J A, Vosko S H, Jackson K A, Pederson M R, Singh D J and Fiolhais C 1992 Phys. Rev. B **46** 6671-87

[45] Rousse G, Rodriguez-Carvajal J, Patoux S and Masquelier C 2003 Chem. Mater. **15** 4082-90

[46] Li J, Yao W, Martin S and Vaknin D 2008 Solid State Ionics **179** 2016-9

[47]Rissouli K, Benkhouja K, Ramos-Barrado J R and Julien C 2003 Mat. Sci. Engin. B **98** 185-9

[48] Molenda J, Ojczyk W, Swierczek K, Zajac W, Krok F, Dygas J and Liu R 2006 Solid State Ionics **177** 2617-24

[49] Dong Y, Wang L, Zhang S, Zhao Y, Zhou J, Xie H and Goodenough J B 2012 J. Power Sources **215** 116-21

[50] Lee J, Pennycook S J and Pantelides S T 2012 Appl. Phys. Lett. **101** 033901

[51] Zhou F, Kang K, Maxisch T, Ceder G and Morgan D 2004 Solid State Commun. **132** 181-6

[52] Guo X, Wang M, Huang X, Zhao P, Liu X and Che R 2013 J. Mater. Chem. A **1** 8775-81

[53] Li Z, Wu S, Wang Z and Fu Y Q 2016 J. Alloy. Compd. **672** 155-60

[54] Vineyard G H 1957 J. Phys. Chem. Solids **3** 121-7

Table I Optimized lattice constants for olivine type $LiFePO_4$ and $LiMnPO_4$ (Å)

		a	b	c	Reference
$LiFePO_4$	Present	4.66	5.92	10.13	
	Exp.	4.69	6.00	10.33	[10]
	Cal.	4.69	6.01	10.33	[43]
$LiMnPO_4$	Present	4.68	6.02	10.36	
	Exp.	4.75	6.11	10.45	[10]
	Cal.	4.74	6.10	10.46	[43]

Table II Strain (%) at the interface between $LiFePO_4$ and $LiMnPO_4$, in which positive and negative values denote compressive and tensile strains.

	(100)		(010)		(001)	
	b	c	a	c	a	b
$LiFePO_4$	0.84	1.14	0.21	1.14	0.21	0.84
$LiMnPO_4$	-0.83	-1.11	-0.21	-1.11	-0.21	-0.83

Table III Calculated energy barriers (E_{diff}) and diffusion coefficients (D) in the bulk $LiFePO_4$, $LiMnPO_4$ and their interfaces.

		E_a/(eV)	D/(cm^2/s)
Bulk	$LiFePO_4$	0.48	7.77×10^{-12}
	$LiMnPO_4$	0.60	7.49×10^{-14}
Interface	(001)-A	0.55	5.18×10^{-13}
	(010)-B	0.45	2.48×10^{-11}
	(010)-C	0.60	7.49×10^{-14}
	(100)-D	0.49	5.28×10^{-12}
	(100)-E	0.44	3.65×10^{-11}

Lists of figure captions:

Figure 1 Crystallographic structures of the bulk (a) $LiFePO_4$ and (b) $LiMnPO_4$. Green, red, gray, yellow and purple balls refer to Li, O, P, Fe and Mn atoms, respectively.

Figure 2 Crystallographic structures of (a) (001), (b) (010) and (c) (100) interfaces between $LiFePO_4$ and $LiMnPO_4$.

Figure 3 (a) Diffusion energy curves of Li in bulk $LiFePO_4$ and $LiMnPO_4$ and in the three interfaces. The diffusion paths are show for (b) (001), (c) (010) and (d) (100) interfaces.

Figure 4 The partial density of states of bulk (a) $LiFePO_4$, (b) $LiMnPO_4$, (c) (100), (d) (010) and (e) (001) interfaces.

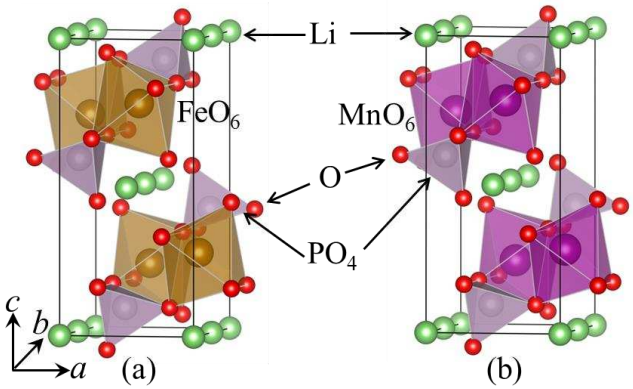

J.J. Shi et al. Figure 1

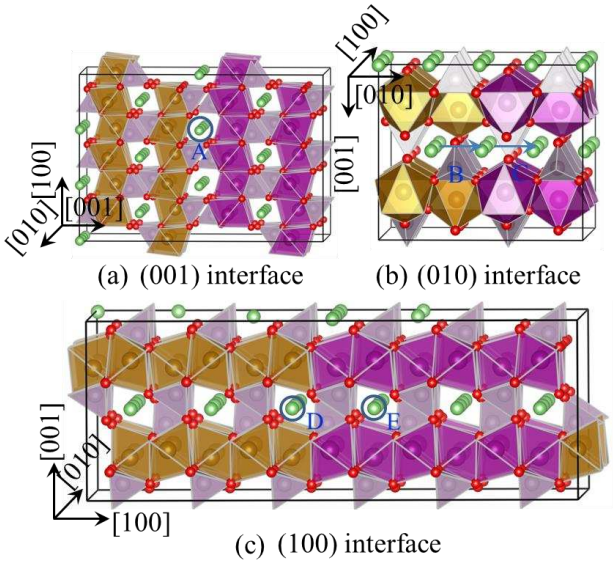

J.J. Shi et al. Figure 2

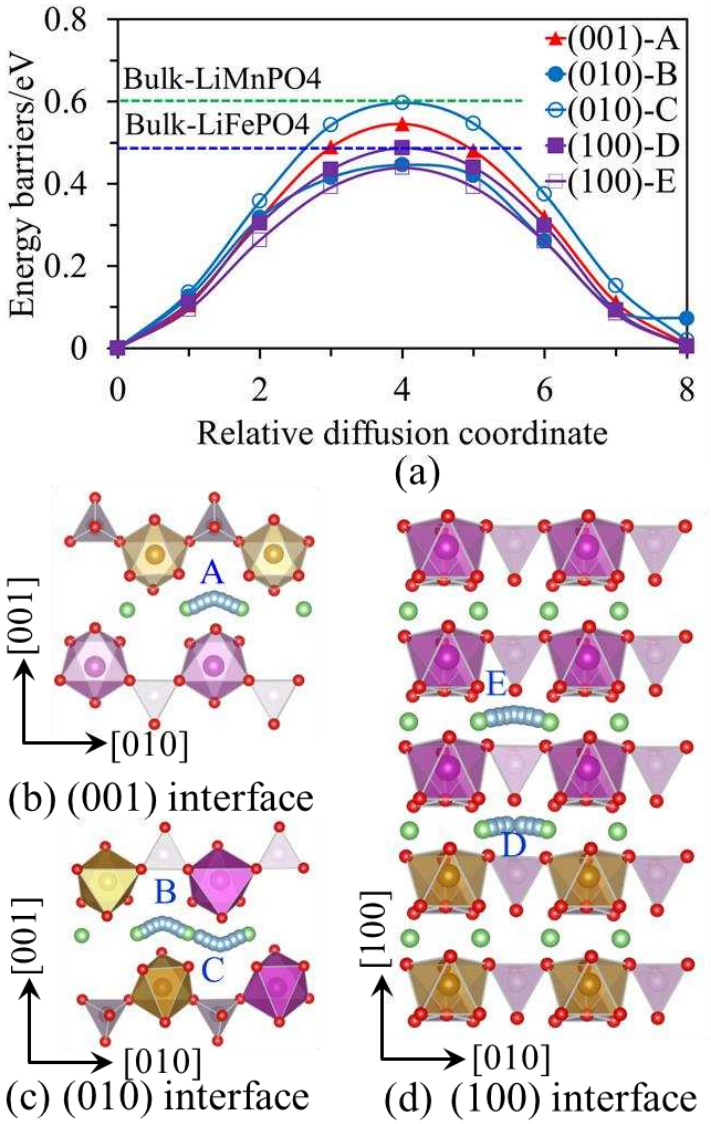

J.J. Shi et al. Figure 3

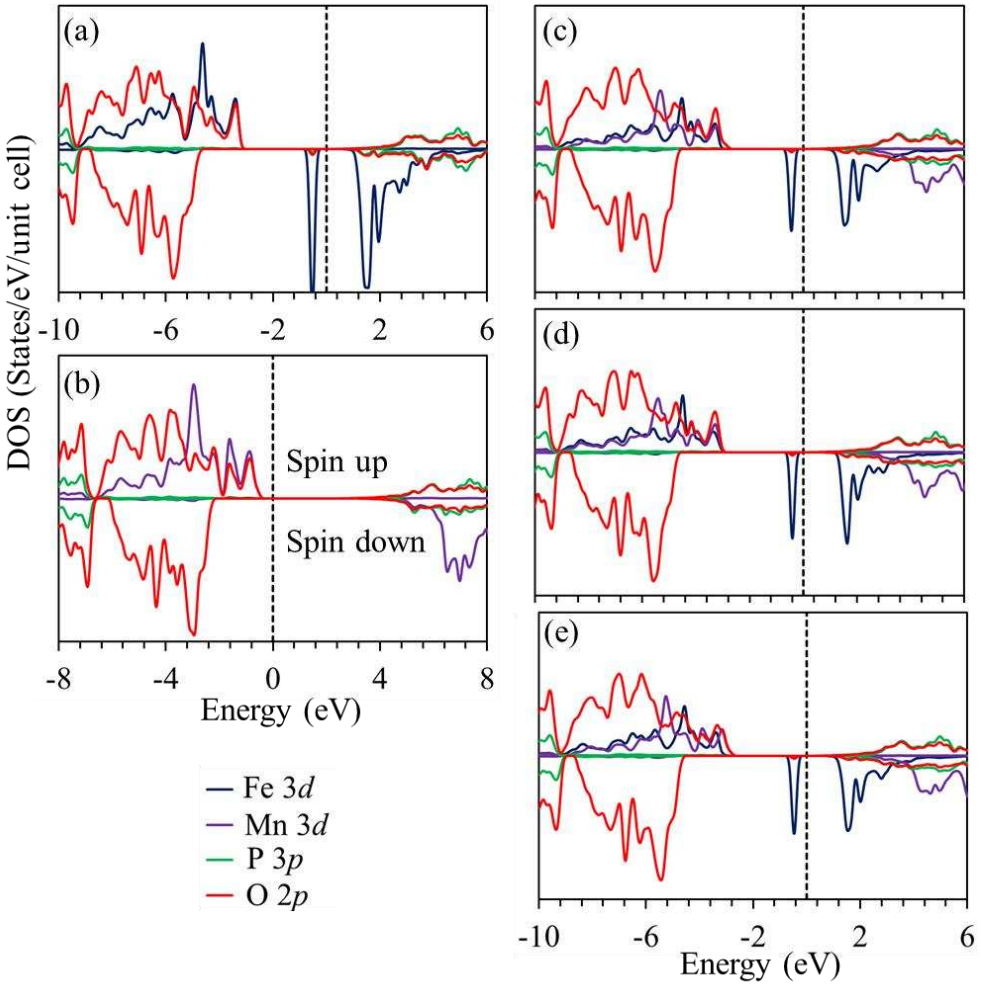

J.J. Shi et al. Figure 4